Structural Aspects of Nanocrystals of Transition-Metal Hexafluorides

James W. Hovick† and Lawrence S. Bartell*

Department of Chemistry, University of Michigan, Ann Arbor, Michigan 48109

Received: July 3, 1997; In Final Form: October 22, 1997

Experiments carried out under systematically changing conditions were performed to generate nanocrystals of MoF_6 and WF_6 in supersonic expansions of the vapor. Results were monitored by electron diffraction. Under warmer expansion conditions the bcc crystals produced rapidly transformed to a metastable monoclinic phase unknown in the bulk, whereas nucleation at colder temperatures led directly to the orthorhombic phase generally considered to be the stable low-temperature allotrope. When nucleation was postponed until the flow was very cold, the orthorhombic diffraction pattern appeared but was mixed with a pattern that could not be identified with any known phase of any hexahalide. Although the evidence is not absolutely conclusive, we believe that a new phase was formed. If this is true, it is an open question whether the phase is another metastable allotrope owing its existence to the kinetics rather than the thermodynamics of formation or whether it, rather than the orthorhombic structure, constitutes the actual low-temperature phase of transition-metal hexafluorides. Cell constants of the recognizable nanocrystals were determined to ascertain whether size effects or effects of the kinetics of growth play a role. Lattice constants of 10 nm crystals of the orthorhombic phase formed in microseconds were indistinguishable from those of the bulk. Variations among the shapes of orthorhombic cells of the various hexafluorides were analyzed and found to be related to the temperature, the bond polarity, and the bond length.

Introduction

At atmospheric pressure the octahedral hexahalides (AX_6) exist in a variety of solid-state forms, including body-centered cubic, rhombohedral, trigonal, monoclinic, and orthorhombic.[1−19] Transition-metal hexafluorides (A = Mo−Rh, W−Pt) in the bulk have only been seen as body-centered cubic, just below the freezing point, and orthorhombic, at lower temperatures.[1−8] Recently, however, it was predicted that these compounds might be induced to transform from body-centered cubic into a monoclinic form exhibited by the chalcogen hexafluorides if they were cooled rapidly.[20] Electron diffraction studies of nanocrystals of MoF_6 and WF_6 approximately 10 nm in diameter, generated by condensation of vapor in a cooling supersonic flow, confirmed this prediction.[21] The behavior of submicroscopic particles of these substances was found to be almost indistinguishable from that of comparable TeF_6 aggregates grown under the same flow conditions.[14] In the present research, nanocrystals of the transition-metal compounds were produced over a rather wide range of expansion conditions. In the course of experiments it was found under conditions of nucleation at lower temperatures than previously examined that the diffraction pattern changed over the entire range examined. Moreover, the resultant profile of intensity could not be reproduced by any combination of known phases. It was not possible, however, to identify the structure of what we believe is a new phase from the diffraction information alone. Diffraction patterns of crystals only 10 nm in diameter are quite diffuse, and much of the pattern was obscured by diffraction from coexisting crystals of the orthorhombic phase.

In view of the opportunity offered by the present technique of studying phases not accessible to conventional methods of crystallography, it was considered worthwhile to determine lattice parameters of 10 nm crystals of the metastable monoclinic phase with some precision. For comparison, and to examine the possibility of effects of particle size and kinetics of formation on structure, the cell constants of 10 nm crystals of the orthorhombic phase were also determined and analyzed. In addition, a procedure is suggested for narrowing the set of possible structures associated with the new pattern from the incomplete information available.

Experimental Section

Samples of gaseous molybdenum hexafluoride (Noah Chemicals, stated purity 99.9%, and Ozark-Mohoning, >99%) and of tungsten hexafluoride (Air Products, 99.9%) were mixed in various proportions with the carrier gas neon (Cryogenic Gas, 99.99%) or, in some cases, with helium or argon (both from Air Products, 99.999%) for introduction into the diffraction chamber of an electron diffractometer described elsewhere.[22,23] Experiments were carried out in pulsed mode to eliminate interference from background gas.[23] Sizes of the nanocrystals produced were inferred in the usual way[24] from breadths of the diffraction rings. Lines we attribute to a new phase appeared when the mole fraction of subject gas was reduced to 0.03 and became more intense the lower the stagnation pressure. Characteristic dimensions of the supersonic nozzles used are listed in Table 1. Representative experimental conditions investigated and corresponding results are given in Table 2. A complete set of runs is documented elsewhere.[24]

Results

Nanocrystals of MoF_6 and WF_6. Orthorhombic and monoclinic nanocrystals of MoF_6 and WF_6 yielded diffraction patterns closely resembling those of their previously studied TeF_6

† Present address: Department of Chemistry, University of North Carolina at Charlotte, Charlotte, NC 28223.

S1089-5647(97)02183-4 CCC: $15.00
Published on Web 01/15/1998

TABLE 1: Dimensions of the Various Nozzles Used in the Supersonic Expansions

nozzle	throat diam, mm	exit diam, mm	length, mm
No. 6	0.13	1.90	30.0
No. 19	0.20	2.03	20.8
No. 30	0.17	1.17	15.2
No. 31	0.18	0.60	9.3

TABLE 2: Selected Results of Supersonic Expansions with Neon Carrier Gas[a]

subject	subject mole fraction	P_{tot}[b]	solid phase[c]
MoF_6	0.30	2.1	m
	0.20	3.4	m
		2.8	m
		2.4	m
		2.0	m
		1.7	o
	0.12	2.8	m
		2.4	m
		2.1	m
		1.7	o + m
		1.4	o
	0.06	3.6	o
		3.1	o
		2.1	o
	0.03	4.1	o
		3.1	o
		2.8	o + u
		1.7	o + u
WF_6	0.20	5.2	m
		4.1	m
		3.1	m
		2.8	o + m
		2.1	o
	0.12	4.1	m
		3.1	o + m
		2.1	o
	0.06	8.3	m
		6.2	o + m
		5.2	o
		4.1	o
		3.1	o
		2.1	o
	0.03	8.3	o
		6.2	o
		5.1	o
		4.1	o

[a] Nozzle No. 31. For nozzle dimensions, see Table 1. Distance from nozzle exit to electron beam, 15 mm. The phase(s) produced depended upon nozzle characteristics as well as mole fraction and pressure. For WF_6 results with a different nozzle, see Figure 4. [b] Stagnation pressure, in bar. [c] m = monoclinic, o = orthorhombic, and u = new unidentified phase.

counterparts[14] as illustrated in Figures 1 and 2. The orthorhombic phase (Figure 1) is grown in the cold flow produced when pressures and/or subject gas mole fractions are comparatively low. If they are high, nucleation is initiated earlier in the flow at warmer temperatures, and the bcc phase is generated, instead, which transforms in microseconds to the metastable monoclinic phase in the cooling expansion. Despite the fact that the monoclinic nanocrystals are less stable than the orthorhombic,[20] they have never been observed to relax to orthorhombic during even the longest times of flight characteristic of the supersonic experiments. This is because the reorganization required in the transition from bcc to monoclinic is minor, but that from monoclinic to orthorhombic is substantial.

The orthorhombic structure belongs to space group *Pnma* with $Z = 4$ as found by Levy et al.[3,6] and the monoclinic to *C*2/*m* with $Z = 6$.[16] It seemed worthwhile to compare the lattice

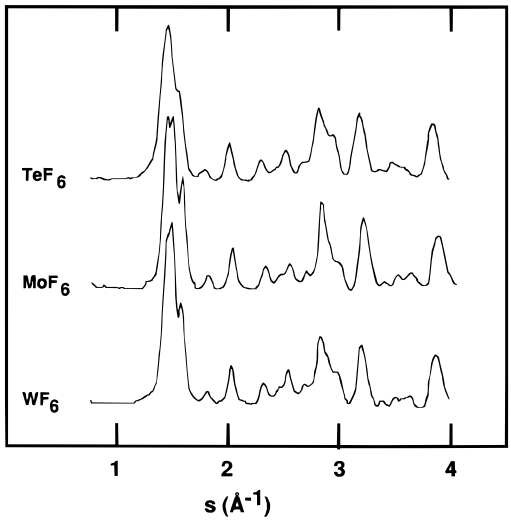

Figure 1. Leveled electron diffraction patterns of 10 nm nanocrystals of orthorhombic TeF_6, MoF_6, and WF_6 produced by condensation of vapor in supersonic flow. Upper trace: subject mole fraction, X_s = 0.06 in Ne, stagnation pressure, 5.5 bar, nozzle No. 6. Middle trace: subject mole fraction, X_s = 0.12 in Ne, stagnation pressure, 2.8 bar, nozzle No. 30. Lower trace: subject mole fraction, X_s = 0.06 in Ne, stagnation pressure, 3.1 bar, nozzle No. 30. For nozzle dimensions see Table 1.

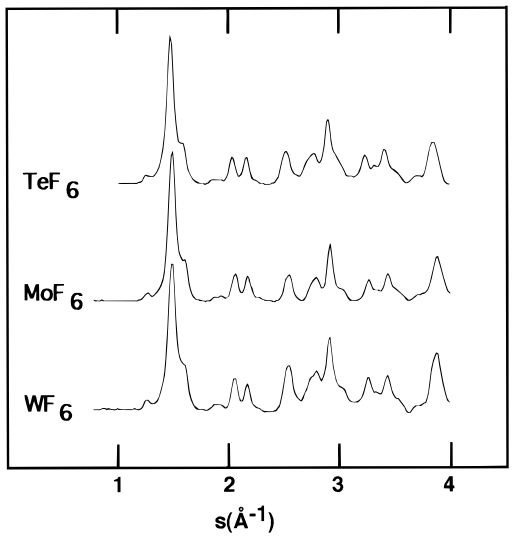

Figure 2. Leveled electron diffraction patterns of 10 nm nanocrystals of monoclinic TeF_6, MoF_6, and WF_6 produced by condensation of vapor in supersonic flow. Upper trace: subject mole fraction, X_s = 0.067 in Ne, stagnation pressure, 7.2 bar, nozzle No. 6. Middle trace: subject mole fraction, X_s = 0.20 in Ne, stagnation pressure, 3.4 bar, nozzle No. 19. Lower trace: subject mole fraction, X_s = 0.12 in Ne, stagnation pressure, 6.2 bar, nozzle No. 19. For nozzle dimensions, see Table 1.

constants of the 10 nm crystals with each other and with those of bulk crystals to find whether any significant differences could be detected. For this purpose the diffraction patterns were analyzed with the aid of the program POWDRFIT.[25] This program attempts to fit an experimental profile of scattered intensity by a sum of peaks generated from the computed structure factor for the cell in question. Peak breadths are modified to take into account the finite size of the crystals involved (assumed to be spherical). Lattice constants are refined by a least-squares procedure requiring no explicit assignment to be made of the Miller indices of experimental peaks. Properly applied, the procedure avoids false minima and offers the advantage that overlapping reflections associated with the rather

TABLE 3: Cell Parameters for Orthorhombic Nanocrystals and Bulk Crystals[a]

subject	*T*, K	*a*[a]	*b*[a]	*c*[a]
TeF_6 nanocrystal[b]	125 ± 5	9.671(22)	8.687(3)	5.048(12)
TeF_6 bulk[c]	15	9.5208(3)	8.6082(4)	4.9991(2)
TeF_6 bulk[c]	190	9.790(1)	8.780(10	5.114(1)
MoF_6 nanocrystal[d]	159 ± 5	9.480(11)	8.600(2)	4.993(8)
MoF_6 bulk [e]	193	9.559(9)	8.668(8)	5.015(5)
WF_6 nanocrystal[f]	163 ± 5	9.537(13)	8.652(2)	5.026(9)
WF_6 bulk[g]	193	9.603(3)	8.713(4)	5.044(3)

[a] Lengths, Å, temperatures, K. Nanocrystal temperatures from ref 26. [b] Intensity data from ref 14, initial mole fraction and pressure, 0.06 in neon at 5.5 bar, nozzle No. 6. [c] Reference 17. [d] This work. Initial mole fraction and pressure, 0.13 in neon at 2.8 bar, nozzle No. 30. [e] Reference 3. [f] This work. Initial mole fraction and pressure, 0.06 in neon at 3.1 bar, nozzle No. 31. For details about nozzles used, see Table 1.

TABLE 4: Lattice Constant Ratios for Orthorhombic Hexafluorides[a]

subject	*T*, K	*a*/*b*	*a*/*c*	*b*/*c*	charge on A
TeF_6 nanocrystal[a]	125	1.113(3)	1.916(6)	1.721(4)	1.22
TeF_6 bulk[b]	15	1.1060(1)	1.9045(1)	1.7219(1)	
TeF_6 bulk[b]	190	1.1151(2)	1.9144(3)	1.7168(3)	
MoF_6 nanocrystal[a]	159	1.102(1)	1.899(4)	1.722(3)	1.65
MoF_6 bulk[c]	193	1.103(1)	1.906(3)	1.728(2)	
MoF_6 bulk[d]	237	1.093(3)	1.895(8)	1.726(8)	
WF_6 nanocrystal[a]	163	1.102(2)	1.898(4)	1.721(3)	1.56
WF_6 bulk[e]	193	1.103(1)	1.904(1)	1.727(1)	
WF_6 bulk[d]	253	1.099(3)	1.902(8)	1.731(8)	
ReF_6 bulk[d]	251	1.097(3)	1.899(8)	1.731(8)	1.66
UF_6 bulk[f]	193	1.103(2)	1.903(3)	1.724(3)	2.02
UF_6 bulk[d]	293	1.108(2)	1.909(3)	1.723(2)	
hcp F's	0	1.0887	1.8851	1.7321	
hcp A's	0	1.0607	1.7321	1.6330	

[a] Nanocrystal studies, this work; bulk, neutron diffraction. Charge on central atom in fractions of an electron (absolute magnitude of) from ref 29. [b] Reference 17. [c] Reference 3. [d] Reference 1. [e] Reference 6. [f] Reference 5. [g] Reference 2.

broad Debye−Scherrer diffraction lines are not troublesome. Extreme accuracy of atomic coordinates is not essential in refinements of lattice constants, but a good estimate of the coordinates is helpful. This estimate can come either from packing calculations or from previous structural studies.

Orthorhombic Phase. Even though the diffraction patterns are diffuse because of the small size of the crystals (∼10 nm), they correspond so well to powder patterns of much higher resolution published for macroscopic crystals of all three substances that there is no doubt about the identities of the phases.[1−12,17] Initial atomic coordinates for orthorhombic nanocrystals of MoF_6 and WF_6 came from refs 3 and 6, and those for TeF_6 came from ref 17. Lattice constants derived for the orthorhombic phases of TeF_6, MoF_6, and WF_6 are listed in Table 3. Ratios of lattice constants can be expected to be less sensitive to temperature and composition than the constants themselves. Such ratios for our electron diffraction patterns are compared with those of the bulk for a number of hexafluorides in Table 4. Temperatures of the nanocrystals estimated as described elsewhere[26] are listed in both tables.

Monoclinic Phase. Conventional crystallography has been unable to carry out analyses of the monoclinic phase of the three compounds reported here, and therefore, a comparison of bulk crystals with the present nanocrystals cannot be made. However, diffraction intensities for crystals of all three substances formed in supersonic jets are so similar to those of SF_6, for which both high-resolution neutron diffraction patterns of the bulk and patterns of nanocrystals have been published,[15,16] that the assignments of phase are unequivocal. Lattice constants for the monoclinic form determined from POWDRFIT analyses are listed in Table 5. The lattice constants listed for TeF_6 have been transformed from values reported by Bartell and Caillat.[25] The lattice was originally identified as triclinic, but it was subsequently shown[16] that a simpler (monoclinic) assignment of a unit cell can be made for the same structure. Atomic coordinates for refinements of the monoclinic structures came from packing calculations by Kinney.[27]

TABLE 5: Cell Parameters for Monoclinic Nanocrystals

subject	*a*[a]	*b*[a]	*c*[a]	*β*[a]
TeF_6[b]	14.67(7)	8.72(3)	5.06(3)	95.12(30)
MoF_6[c]	14.314(12)	8.606(2)	5.021(6)	95.93(9)
WF_6[d]	14.301(26)	8.631(4)	5.035(12)	96.43(20)

[a] Lengths, Å; angles, deg. [b] This structure was originally indexed in ref 26 in terms of a triclinic lattice. [c] Nucleated from mole fraction 0.20 in neon carrier, stagnation pressure 3.4 bar, nozzle No. 19. [d] Nucleated from mole fraction 0.12 in neon carrier, stagnation pressure 6.2 bar, nozzle No. 19.

Estimates of temperatures of the monoclinic particles cannot be made as directly as they were for the orthorhombic because no information is available about lattice constants as a function of temperature. An alternative estimate in terms of the evaporative cooling temperature[28] can be made crudely. Since the monoclinic phase has not yet been observed in the bulk, no experimental vapor pressure data exist to calculate this temperature. Nevertheless, the known metastability of the monoclinic form relative to the orthorhombic[20] implies that the monoclinic form has a slightly higher vapor pressure than the orthorhombic and, therefore, that the evaporative cooling temperature is slightly lower for the monoclinic nanocrystals. Hence, we infer that the monoclinic clusters of TeF_6, MoF_6, and WF_6 reaching the electron beam in the current experiments are a few degrees lower than 125 K for TeF_6, 168 K for MoF_6, and 153 K for WF_6.

Considerations of the Proposed New Phase. As mentioned in the previous section, what we interpret to be an unknown phase of both MoF_6 and WF_6 is produced in supersonic flow when nucleation takes place under even colder conditions than those leading to the orthorhombic phase. Changes in the diffraction intensities appeared when the mole fraction of subject gas was reduced to 0.03 and the carrier gas pressure was decreased. The most conspicuous feature of the altered diffraction pattern is the appearance of a strong new peak at $s \approx 3.7$ Å^{-1}. In addition, as the intensities of the orthorhombic peaks decrease with changing expansion conditions, most notably those at 1.8, 2.0, 2.3, 2.5, and 2.9 Å^{-1}, the 2.8 Å^{-1} peak grows and the shape of the 1.5 Å^{-1} peak is markedly altered. Figures 3 and 4 illustrate these changes as the stagnation pressure is reduced. Attempts to identify possible structural changes responsible for the new features of the pattern were severely hampered by the presence of a substantial concentration of the orthorhombic phase.

Discussion

Lattice Constants. Lattice constants of the nanocrystals in Table 3 appear to differ from those of the bulk by no more than might be expected from the temperature differences. For this reason one method adopted in ref 26 for estimating temperatures of particles in supersonic beams was to infer them from lattice constants by a suitable nonlinear interpolation. Temperatures so derived agreed quite well with those deduced

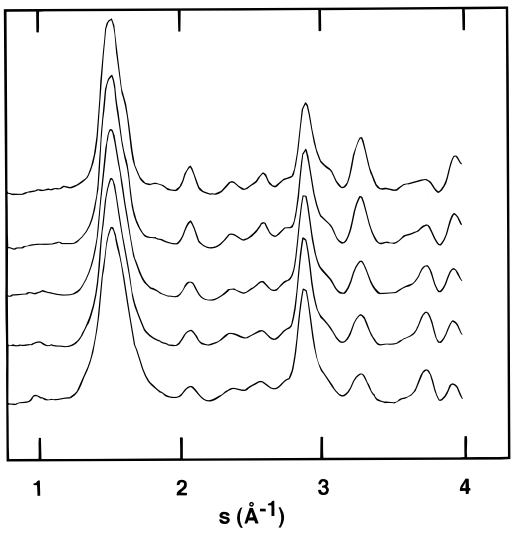

Figure 3. Leveled electron diffraction patterns of nanocrystals of MoF_6 generated in supersonic expansion through nozzle No. 31 with X_s = 0.03 in Ne. Stagnation pressures, in bar, from top to bottom are 3.1, 2.8, 2.1, 1.7, and 1.4. For nozzle dimensions, see Table 1.

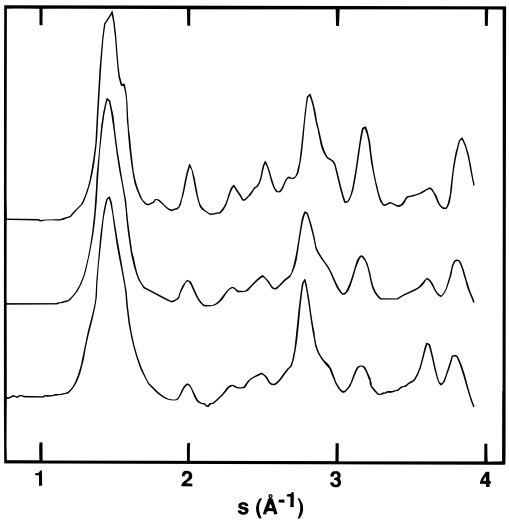

Figure 4. Leveled electron diffraction patterns of nanocrystals of WF_6 generated in supersonic expansion through nozzle No. 6 with X_s = 0.03 mol in Ne. Stagnation pressures, in bar, from top to bottom are 6.2, 4.1, and 3.1. For nozzle dimensions, see Table 1.

from the temperature calculated for an evaporative ensemble.[26] Lattice ratios in Table 4 offer an alternative comparison free from scale factors related to temperature and molecular size. Lattice ratios for the nanoparticles are very close to those for the same material in the bulk, deviating by scarcely more than the estimated uncertainties. Because a mixture of phases was observed under some experimental conditions, it was decided to find whether the subtraction of various amounts of the pattern of the monoclinic phase or of the presumed new phase would give lattice ratios agreeing even more closely with those of the macroscopic crystals. It was found that the agreement deteriorated in proportion to the assumed concentration of contaminant. Therefore, we conclude that the clusters selected for Table 3 were not significantly contaminated by another phase.

Systematic shifts in the lattice constants might be expected from variations in the temperature, the electrostatic interactions, and the molecular bond lengths. Only for the neutron diffraction study of bulk TeF_6[17] is the accuracy high enough to establish with precision the magnitude of all of the temperature shifts. Taking these shifts into account of course necessarily improves the comparison of lattice constants between nanoparticles and the bulk (because temperatures were inferred from the cell constants) and marginally improves the already good agreement between lattice constant ratios. We conclude that, to within experimental accuracy, there is no distinction between the packing of molecules in 10 nm crystals formed in microseconds and those annealed for extended times in the bulk.

The entries in Table 4 form a convenient series for testing effects of ionic character because, to better than 1%, all of the molecules (except for UF_6) are of the same size. Crystal packing calculations by Kinney[29] show that increasing the partial charges on the atoms (while retaining neutrality of the molecules) tends to decrease the a/b and a/c ratios but to increase the b/c ratio slightly. This trend is borne out in the comparisons in Table 4 where estimated charges on the central atoms are tabulated, as deduced from electronegativity by a method described elsewhere.[29,30] The compound with the most polar bonds, UF_6, does not follow this trend, perhaps because its bonds are decidedly longer than those of the other entries.

A feature helping to stabilize the molecular packing in the orthorhombic phase is the organization of fluorine atoms into what is nominally a double hexagonal close-packed array (stacking ABACAB...).[31−33] A similar feature also characterizes the monoclinic phase (which enjoys a nominally hcp arrangement of fluorines) but not the bcc phase which is stabilized by entropy. If the fluorines were actually packed into an ideal hcp lattice (unique direction along the orthorhombic x axis), the corresponding lattice ratios can be calculated. Such ratios are listed near the bottom of Table 4. If, alternatively, AF_6 molecules were envisaged as quasispherical, close-packed entities, the hcp array of A atoms would have its unique direction along the y axis of the orthorhombic lattice, with corresponding lattice ratios as shown in the last entry of Table 4. It is clear that the observed ratios are in considerably better agreement with the ratios for the idealized close packing of fluorines than with the ratios for hypothetical AF_6 molecules packing as spheres. It might at first glance be supposed that UF_6 would be a particularly good example of close packing of fluorines because its intramolecular F−F distances are nearly identical with the intermolecular van der Waals F−F distance whereas the other tabulated examples have appreciably shorter intramolecular than intermolecular F−F distances.[5] Table 4 shows that ratios for UF_6 are no closer than those for the smaller molecules to the idealized packing of fluorines. Why this should be so is unclear. A contributing factor may be that the crystal environment distorts the UF6 octahedra[5] by far more than it does those of the more rigid, more covalent octahedra of the smaller molecules.[15−17]

Because no bulk samples of the monoclinic phase of any of the tabulated substances have yet been produced, it is not possible to generate the detailed comparisons made above. It is likely that such samples could be prepared if the bcc phase were cooled sufficiently rapidly and quenched to low temperatures.

An Approach To Analyzing the Altered Intensity Profile. The diffraction pattern characterizing what we interpret as a new phase is too badly obscured by the coexisting orthorhombic phase to allow a detailed characterization. Nevertheless, we believe that the changes in diffraction patterns with expansion conditions are real and sufficiently consistent to warrant the claim of a new phase. Results cannot be attributed to a simple contaminant introduced fortuitously because the characteristic changes were encountered for a given substance with the same sample simply by changing the stagnation pressure, and they occurred in the same way for WF_6 as for MoF_6. Unfortunately,

no sample of TeF_6 was available to find whether this compound behaved similarly.

Even though the new features of the diffraction pattern accompanying the lowering of the nucleation temperature were seriously obscured, the observed information does rule out many possibilities, as will be discussed below. It is fair to point out that referees of this paper believed that the evidence cited in favor of a new phase is unconvincing. They suggested that the most striking new feature in our patterns, the strong 3.7−3.8 $Å^{-1}$ peak we attributed to the new phase, might alternatively be explained by a high-order reflection from the orthorhombic phase that, by chance, is extremely sensitive to small changes in the structure. Although we saw no great sensitivity of synthesized diffraction intensities to shifts in cell constant ratios (which can cause several reflections to overlap and amplify a peak height), to large changes in relative Debye−Waller factors of the atoms, or to the substitution of tungsten for molybdenum (considerably enhancing the scattering amplitude at the metal site), we carried out extensive tests of the referees' suggestion. Changes in intensity were calculated for shifts in molecular positions and orientations allowed in the *Pnma* space group. Allowed translations are governed by just two coordinates. When these were altered systematically over a grid corresponding to displacements from optimal packing and extending to over 0.4 Å in all directions in the planes with constant *y* (which displacements led to severe steric conflicts) and angles up to ∼0.3 rad, no patterns in acceptable accord with observations were found. Although some displacements did, indeed, lead to a strong peak at 3.7 $Å^{-1}$, other features associated with these displacements were totally at variance with observations. On the other hand, it was suggested by another referee that the rather large changes in intensities might be due to surface effects associated with the smaller crystals that might result from the reductions in the stagnation pressure. Although such changes had been seen in studies of SF_6 carried out at Orsay,[34] they were encountered for clusters considerably smaller than those obtained in the present supersonic expansions through Laval nozzles. Moreover, because the breadths of the diffraction rings in the pertinent series of experiments did not reveal a major change in the mean size of the crystals formed, such a surface effect can be ruled out.

Although it is beyond the scope of the present paper to analyze the problem in detail, it is worthwhile to point out a possible approach to the identification of a new phase if such a phase is present. First should be considered the various structures into which octahedral molecules might reasonably be expected to pack. Besides the known bcc, orthorhombic, and monoclinic structures are the trigonal and rhombohedral structures that certain hexachlorides adopt[18,19] as well as a number of other possibilities to be mentioned below. For the hexafluorides reasonably realistic interaction potential functions exist, calibrated to make the computed diffraction patterns of known phases reproduce the observed patterns.[28,29] Therefore, it is possible to carry out crystal packing calculations for the proposed crystal structures to find whether the corresponding diffraction patterns can account for the features seen in the present experimental patterns. It is not just the intensity of a single peak that characterizes the observed changes in pattern; it is the entire profile of intensity that must be reproduced by a single phase or mixture.

To investigate plausible structures in addition to the trigonal and rhombohedral structures, we constructed several other molecular packings with close-packed planes of fluorines. In all, we found a dozen different crystal structures comparable in packing energy with the known structures before we became aware of Müller's systematic analysis of potentially stable hexahalide structures.[31−33] Several of our candidates turned out to be new, not listed among those proposed by Müller. Among the dozen structures whose diffraction patterns were calculated, a 3.7 $Å^{-1}$ peak of sufficient intensity to account for the new phase was found only for the rhombohedral structure and a heretofore never seen orthorhombic structure, space group *Pbam* (No. 55) with $Z = 8$ molecules per unit cell. Certain aspects of the synthetic intensity curves at intermediate diffraction angles weighed against their acceptance, however. On the other hand, a variety of alternative, low-energy monoclinic, trigonal, and orthorhombic structures could be definitively ruled out despite the fact that their calculated stabilities were quite competitive with those of the known phases. Their associated diffraction patterns were clearly incompatible with our observations. Details of this work will be presented at the completion of computations now in progress to narrow the list of candidates for the postulated new phase.

It is worthwhile to ask whether the proposed new phase, if it exists, might simply be a metastable phase or whether it might actually be the stable phase at very low temperatures. In either case the role of kinetics would play a crucial role. It might be supposed that a new phase could be an artifact of the kinetics of condensation of vapor at very cold temperatures. For example, the condensation of dimethylacetylene in supersonic expansions leads to a clearly metastable crystal structure unknown in the bulk.[35] Times of formation of the clusters in our supersonic experiments (microseconds) are fleeting in comparison with the times involved in crystal structure determinations by X-ray and neutron diffraction (hours to days). From this it might be imagined that only the X-ray and neutron studies allow enough time to achieve true equilibrium. This is not necessarily the case. Even in our molecular dynamics simulations carried out on a time scale yet a millionfold briefer than our supersonic experiments, the systems, upon cooling, sometimes undergo spontaneous phase changes leading to the true low-temperature phase.[36] What might prevent the X-ray and neutron diffraction studies of bulk materials from attaining the true equilibrium phase of very cold samples is the fact that the bulk samples necessarily begin with higher temperature crystalline phases. At very low temperatures, phase changes requiring a substantial reorganization of the molecules can become so sluggish that the transformation is experimentally inaccessible. In our supersonic experiments, for example, we have never seen the bcc or metastable monoclinic phases of hexafluorides transform to the more stable orthorhombic phase. But we can and do see the orthorhombic phase if we condense vapor *directly* to this phase at low enough nucleation temperatures. At yet lower nucleation temperatures it is conceivable that we might generate an even lower temperature, stable phase. What our experiments have shown is that the barrier to formation of a phase by nucleation of the vapor can be substantially lower than that for a transformation in the solid state. If the suspected new phase can be confirmed, continuing research may clarify which kinetic basis underlies its existence.

Acknowledgment. This research was supported by a grant from the National Science Foundation. We thank Dr. Kurtis Kinney for carrying out some of the crystal packing calculations.

References and Notes

(1) Siegel, S.; Northrup, D. A. *Inorg. Chem.* **1966**, *5*, 2187.
(2) Taylor, J. C.; Wilson, P. W.; Kelly, J. W. *Acta Crystallogr.* **1973**, *B29*, 7.

(3) Levy, J. H.; Taylor, J. C.; Wilson, P. W. *Acta Crystallogr*. **1974**, *B31*, 398.
(4) Levy, J. H.; Sanger, P. L.; Taylor, J. C.; Wilson, P. W. *Acta Crystallogr*. **1974**, *B31*, 1065.
(5) Taylor, J. C.; Wilson, P. W. *J. Solid State Chem.* **1975**, *14*, 378.
(6) Levy, J. H.; Taylor, J. C.; Wilson, P. W. *J. Solid State Chem.* **1975**, *15*, 360.
(7) Levy, J. H.; Taylor, J. C.; Wilson, P. W. *J. Less-Common Met.* **1976**, *45*, 155.
(8) Taylor, J. C. *Coord. Chem. Rev.* **1976**, *20*, 197.
(9) Michel, J.; Drifford, M.; Rigny, P. *J. Chim. Phys.* **1970**, *67*, 31.
(10) Dolling, G.; Powell, B. M.; Sears, V. F. *Mol. Phys* **1979**, *37*, 1859.
(11) Dolling, G.; Powell, B. M. *Mol. Cryst. Liq. Cryst.* **1979**, *52*, 27.
(12) Dolling, G.; Powell, B. M. *Can. J. Chem.* **1988**, *66*, 897.
(13) Raynerd, G.; Tatlock, G. J.; Venables. J. A. *Acta Crystallogr*. **1982**, *B38*, 1896.
(14) Bartell, L. S.; Valente, E. J.; Caillat, J. C. *J. Phys. Chem.* **1987**, *91*, 2498.
(15) Powell, B. M.; Dove, M. T.; Pawley, G. S.; Bartell, L. S. *Mol. Phys.* **1987**, *62*, 1127.
(16) Cockroft, J. K.; Fitch, A. N. *Z. Krystallogr*. **1988**, *184*, 123.
(17) Bartell, L. S.; Powell, B. M. *Mol. Phys.* **1992**, *75*, 689.
(18) Ketelaar, J. A. A.; Van Oosterhout, G. W. *Recl. Trav. Chim. Pays-Bas* **1943**, *62*, 197.
(19) Taylor, J. C.; Wilson, P. W. *Acta Crystallogr*. **1974**, *B30*, 1216, 1481.
(20) Bartell, L. S.; Xu, S. *J. Phys. Chem.* **1991**, *95*, 8939.
(21) Bartell, L. S.; Hovick, J. W.; Dibble, T. S.; Lennon, P. L. *J. Phys. Chem.* **1993**, *97*, 230.
(22) Bartell, L. S.; Heenan, R. K.; Nagashima, M. *J. Chem. Phys*. **1983**, *78*, 236.
(23) Bartell, L. S.; French, R. J. *Rev. Sci. Instrum.* **1989**, *60*, 1223.
(24) Hovick, J. W. Ph.D. Thesis, University of Michigan, Ann Arbor, MI, 1994.
(25) Bartell, L. S.; Caillat, J. C.; Powell, B. M. *Science* **1987**, *236*, 1463. Bartell, L. S.; Caillat, J. C. *J. Appl. Crystallogr*. **1987**, *20*, 461.
(26) Hovick, J. W.; Bartell, L. S. *J. Mol. Struct*. **1995**, *346*, 231.
(27) Kinney, K. Private communication.
(28) Gspann, J. In *Physics of Electronic and Atomic Collisions*; Datz, S., Ed.; Hemisphere: Washington, DC, 1976. Klots, C. *J. Phys. Chem.* **1988**, *92*, 5864.
(29) Kinney, K.; Bartell, L. S. *J. Phys. Chem.* **1996**, *100*, 15416.
(30) Kinney, K. Ph.D. Thesis, University of Michigan, Ann Arbor, MI, 1995. Note that there are errors in the tabulated quantities and in the labels of figures in the thesis.
(31) Müller, U. *Acta Crystallogr*. *A* **1979**, *35*, 188.
(32) Müller, U. Supplementary Publication No. SUP 33843, British Kending Library.
(33) Willing, W.; Müller, U. *Acta Crystallogr*. **1988**, *B44*, 1.
(34) Torchet, G. *Z. Phys. D* **1991**, *20*, 251.
(35) Huang, J.; Bartell, L. S. *J. Phys. Chem.* **1995**, *99*, 11147.
(36) Chen, J.; Bartell, L. S. *J. Phys. Chem.* **1993**, *97*, 10645.